



Investigation of light emitting diodes using nuclear microprobes

Changyi Yang ^{a,*}, Andrew Bettioli ^c, David Jamieson ^c, Xiao Hua ^b, J.C.H. Phang ^b,
D.S.H. Chan ^b, Frank Watt ^a, T. Osipowicz ^a

^a *Research Center for Nuclear Microscopy, Department of Physics, National University of Singapore, Singapore 119260*

^b *Center for Integrated Circuit Failure Analysis and Reliability, National University of Singapore, Singapore 119260*

^c *Microanalytical Research Centre, School of Physics, University of Melbourne, Parkville 3052, Australia*

Abstract

The quality of semiconductor p–n junctions and substrates is essential for a reliable performance of microelectronic devices. The imaging techniques of ion beam induced charge (IBIC) and ionoluminescence (IL) are applied to image and analyze light emitting diodes (LEDs). The LEDs have been imaged both from the front (beam normal to p–n junction plane) and from the transverse direction (beam parallel to p–n junction plane). The imaging techniques provide details on the structural uniformity of the p–n junction and the light emitting properties, as stimulated by proton irradiation. Following IBIC and IL analysis, PIXE and RBS provide elemental distribution information on the metal layers and other components in the LEDs. The techniques which can be utilized by the nuclear microprobe potentially provide powerful tools for the failure analysis and quality control of the fabrication of microelectronic devices. © 1999 Published by Elsevier Science B.V. All rights reserved.

1. Introduction

The LED is one of most widely used electronic devices. LEDs of different colors can be used for the information indicators in various electronic instruments. They also have important applications in fiber communication, and have a high potential when used as a solid state light source with high efficiency.

LEDs are usually made of III–V compound semiconductors such as GaAsP. By changing the elements that compose the semiconductor and the

ratio of III-group to V-group elements, one can change the characteristics of the LED, including color and brightness. The quality of the LEDs, or in the term of the lifetime and reliability of LEDs, relies on various aspects in the manufacturing processes, such as the process of p–n junction, the crystal growth of p and n-type substrate materials, as well as the formation of metal–semiconductor contacts.

Microscopic methods such as light microscopy and scanning electron microscopy (SEM) are important conventional instruments for failure analysis of the microelectronic device [1]. The cathodoluminescence (CL) technique is also a well-established method in SEMs for semiconductor characterization [2]. The SEM-CL technique has

* Corresponding author. *Present address:* Department of Physics, University of North Texas, Denton, TX, USA. E-mail: cy0011@unt.edu

been widely used for the failure analysis of optoelectronic devices and the characterization of defects [3,4]. The method of electron beam induced current (EBIC) is another highly useful technique in SEMs applied to the characterization of semiconductor materials and fabricated microelectronic devices [5]. The SEMs usually can reveal information to a depth of a few μm only; deep buried structures are not accessible.

In order to improve the manufacturing process of LEDs, microscopic techniques are required to provide structural information from the surface to deep in the device. Nuclear microprobes have a high potential to meet their demands since the high-energy particles make it possible to access much deeper structures than SEMs. The analytical techniques established in nuclear microscopy, including PIXE, RBS, IL and IBIC, are potentially useful techniques for material characterization and failure analysis of microelectronic devices. PIXE is a well-established method for elemental composition analysis [6]. RBS is a highly useful tool for providing stoichiometry and elemental depth profiling information in solids [7]. IBIC can be used to characterize the electronic properties of fabricated device or semiconductor materials [8]. IL can be used to study crystal defects [9,10]. We use these techniques, especially IBIC and IL, to investigate the LEDs and study the quality problems that may be closely related to the potential failures of the LEDs.

2. LED samples and the experimental arrangement

Yellow LEDs with emission wavelength at 585 nm have been investigated using IBIC, IL, PIXE and RBS in a nuclear microprobe. The LEDs were processed with a GaAsP structure grown on a GaP substrate by a vapor phase epitaxy process, and shaped as a 300 μm square with n-type substrates of 180 μm thickness and a p-type top layer of 7 μm thickness. The metal p-contact (aluminum and tungsten alloy) was formed at the top p-type layer in a square shape of 100 by 100 μm size and about 6–8 μm thickness. The n-contacts were formed with Au alloy at the bottom of n-type substrate.

As shown in Fig. 1, LED samples can be mounted in two different geometric arrangements: frontal and side-on imaging. In the mode of frontal imaging, the focused ion-beam penetrates perpendicularly to the p–n junction plane through various layers, including metal p-contact and p/n-type substrates. In the second mode, the side-on surface is subjected to ion-beam scanning. In each of the two options, through the IBIC imaging analysis, the quality of the p–n junction and the substrate materials can be accessed. In the present work the IBIC imaging analysis was carried out without any external bias-voltage to the p–n junctions. The other techniques, including IL, PIXE and RBS, can also be applied together for providing complementary information, such as luminescence properties of the LED substrate and elemental distribution of the different components of the LED.

3. Experimental results and discussion

A yellow light LED was wire-bonded for investigating the p–n junction quality, and the sample made for frontal imaging. The p–n junction was located roughly 6–7 μm below the surface. In order to attain optimal contrast for the IBIC imaging of the junction, a TRIM [11] calculation was carried out to find the best suitable proton energy. The penetration range of 0.8 MeV protons in the LED is about 9.0 μm , which is slightly deeper than the p–n junction location. A sub-micrometric beam at a very low beam current

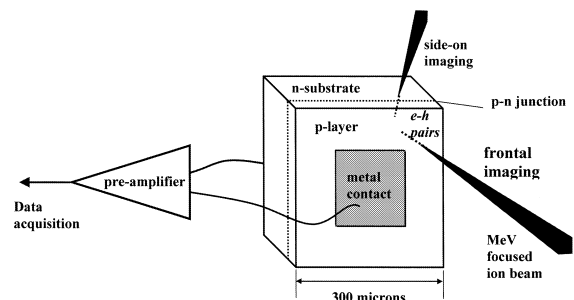


Fig. 1. The layout of LED device structure and the experimental arrangement.

(about 1.6 fA or 10 000 ion/s) was used in the IBIC imaging analysis. The IBIC data were accumulated for about 10 min over an area of 0.132 mm-square. After the IBIC analysis, the p–n junction of the LED remained undamaged, because of the very low beam dose applied. The IBIC results are displayed in Fig. 2. In order to compare the IBIC results with those of SEM-EBIC, EBIC analysis was carried out with 15 keV electron beams after the IBIC analysis. The EBIC image and the secondary electron image are displayed in Fig. 3. The IBIC map displayed in the Fig. 2(a) is obtained by mapping signals located in window (a) indicated in the IBIC spectrum in Fig. 2(c). The map seems to show structural defects close to the device surface, because the defect structures are also found in the EBIC map shown in Fig. 3(a). The IBIC image in Fig. 2(b) is produced by mapping window (b); several dark spots indicate defects in deeper structure not accessible to EBIC.

The excitation depth of an electron beam of 15 keV energy is limited to 3–5 μm ; therefore there is no EBIC signal produced at the p-contact metal layer area. Defects in the shallow p-type layer yield dark areas in EBIC image. The IBIC map shown in Fig. 2(a) also reveals these defects. However, deeply buried defects in the p–n junction and surrounding areas are not accessible by EBIC, but are clearly revealed by the IBIC map shown in Fig. 2(c). These defects shown as dark spots in the IBIC map may be associated with dislocation defects of the original n-type materials, the defects may exist prior to the formation of p–n junction.

The same type of LED (non-wire-bonded) was analyzed by IL imaging. The IL analysis is carried out from the front side using 3.0 MeV protons focused down to about a few μm beam size and 0.1 nA beam current. The IL signal is detected in panchromatic mode with a photomultiplier tube (PMT). The PMT is Hamamatsu R943-02 with a

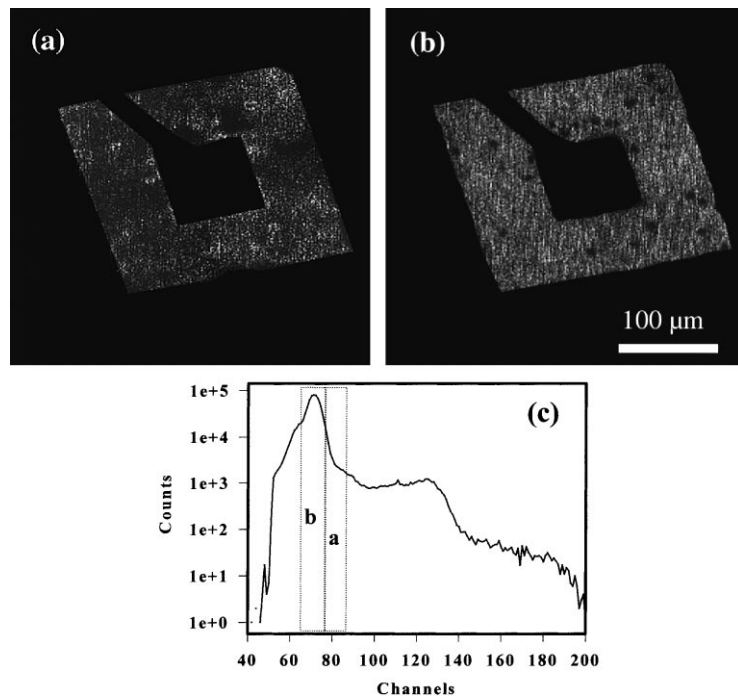


Fig. 2. An LED is investigated using 0.8 MeV proton beams. The IBIC spectrum is displayed in (c). The p–n junction is roughly located 7 μm below the surface. The IBIC map displayed in (a) is obtained by mapping signals located in window (a) indicated in the IBIC spectrum. The map reveals the shallow surface defects. The defects are comparable with those revealed by the EBIC image shown in Fig. 3(a). The IBIC image in (b) is produced mapping window (b); it reveals defects in the p–n junction and deep substrate.

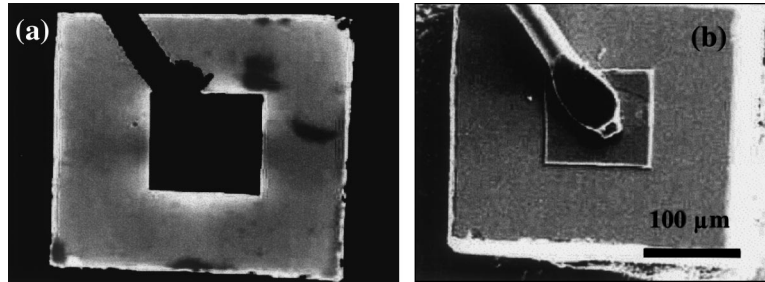


Fig. 3. SEM-EBIC and SEM-SE images of the same LED as investigated in Fig. 2 are obtained with 15 keV electron beams in a scanning electron microscope. The electron beam does not reach the p–n junction. A few dark areas shown in the SEM-EBIC image indicate defects existing in the top p-type layer. The SEM-SE image shows good topographic condition of the LED device.

photocathode 650S (GaAs), which is sensitive at the wavelength from 160 to 930 nm. The PMT is operated in photon counting mode at room temperature with a very high dark current (about 5000 cps). The beam current is kept to be relatively low (100 pA) for IL analysis with a signal-to-noise-ratio about 10 or larger. The IL data were accumulated for about 5–8 min. After IL analysis, PIXE and RBS analysis were carried out with a beam current increased to 1 nA. The imaging re-

sults are displayed in Fig. 4. The elemental maps are obtained by PIXE analysis. The metal contacts were measured by RBS to be 6–8 μm thick. The IL map does not show any obvious defects structure in the p and n-type substrates, but this may be due to low signal-to-noise-ratio and poorer spatial resolution in the IL imaging than that in IBIC imaging due to the use of larger slits in IL measurement. The elemental distribution in the substrate is shown to be homogenous. The Al and W

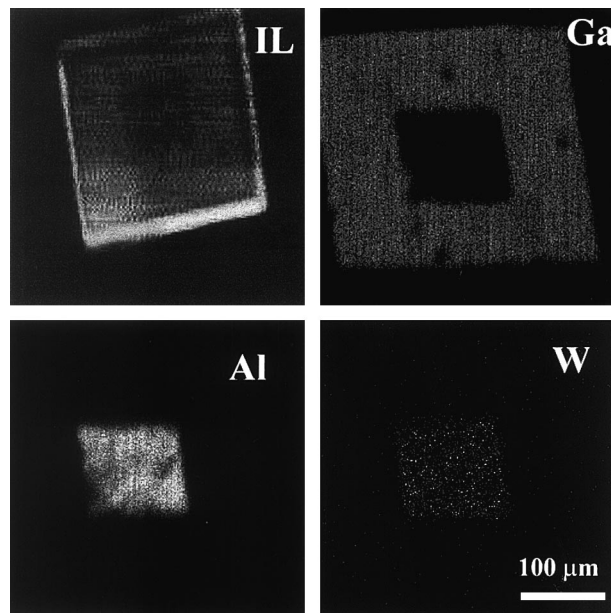


Fig. 4. IL and elemental maps of a yellow light LED (not wire-bonded). The IL map is obtained with a PMT in panchromatic mode and X-ray maps are obtained by PIXE. The slightly stronger intensity of IL at the lower left edge is due to ion beam variation.

maps indicate a partial metal layer damage at an edge during a previous electroluminescence test for a sample selection.

In order to obtain more details of the p–n junction quality, an identical new LED was prepared for the analysis in a side-on arrangement, as shown in Fig. 1. The LED is fixed in resin with its edge upwards and the edge was polished carefully with very fine waterproof silicon carbide paper (FEPA P #4000). The side-on surface was polished down until the p-contact edge reached surface. The polished surface was investigated under an optical microscope and no mechanical distortion was found. A 3.0 MeV protons beam was used for the side-on IBIC analysis. In order to perform large zoom-in imaging, the IBIC imaging area is much smaller than the LED size. Two sections along the p–n junction were chosen for the investigation, one at middle of the p–n junction marked as A and another at the edge marked as B. The results of the IBIC imaging taken from sections A and B are shown in Fig. 5. The IBIC maps of high charge

collection efficiency are displayed on the left side, and the maps of low charge collection efficiency are displayed on the right side of Fig. 5. The p–n junction revealed by IBIC map from section A displays some distortion, possibly indicating imperfections in the junction structure. In section B, the p–n junction does not show such effects. Since the total dose received in the LED for the IBIC analysis is very small (about 100 ions per pixel), the beam damage can be ignored. IL analysis was carried out to further investigate possible crystal defects of the LED substrate using the same PMT as that in the frontal LED imaging. The IL map is displayed in Fig. 6. The IL signal is slightly stronger at the section A where IBIC shows a distorted p–n junction structure than at the normal section B. Defects associated with new color centers, which may have luminescence emission at longer wavelength than the designed emission wavelength (585 nm), might also act as charge trapping centers. The localized charge trapping centers can reduce the IBIC charge collection

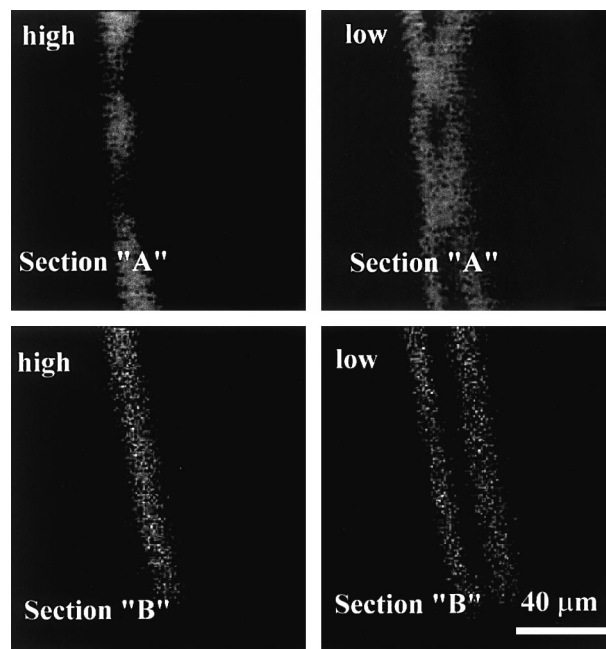


Fig. 5. IBIC images of LED junction using 3.0 MeV protons in a side-on sample mounting. The results of the IBIC imaging taken from sections A and B are displayed. The IBIC maps of high charge collection efficiency are displayed on the left side, and the maps of low charge collection efficiency are displayed on the right side. The p–n junction revealed by IBIC map from section A displays distortion. The same locations are marked as A and B in the IL map shown in Fig. 6.

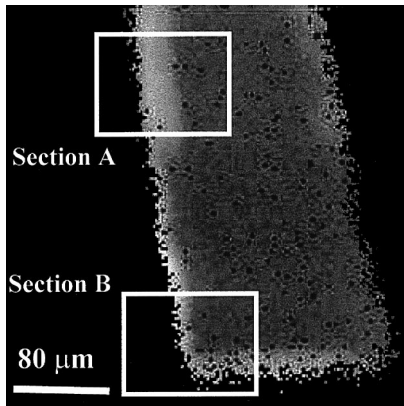


Fig. 6. IL image from the LED in side-on mounting, using 3.0 MeV proton beam. The IL intensity is not homogeneous at the area along the p–n junction direction. There is an increased intensity at the location A where the IBIC image indicates the distortion of p–n junction. The IL shows less intensity at the location B where the IBIC image indicates an undistorted p–n junction.

efficiency, resulting in an inhomogeneity of the p–n junction pattern as revealed by the IBIC image obtained in a side-on experimental arrangement.

4. Conclusion

Nuclear microprobe analysis can provide detailed structural information on LEDs. The quality of the p–n junction and any defects of the substrate layers in shallow to deep depths can be readily revealed by IBIC and IL techniques using ions of optimum energy. The elemental structure of LEDs substrate layers and metal contacts can also be characterized using RBS and PIXE techniques. Nuclear microprobes are useful tools for

the diagnostic analysis of LEDs and other similar types of microelectronic devices.

Acknowledgements

The National Science and Technology Board of Singapore is gratefully acknowledged for the financial support of the present work.

References

- [1] B.P. Richards, P.K. Footner, *The Role of Microscopy in Semiconductor Failure Analysis*, Oxford University Press, Royal Microscopical Society, 1992, pp. 16–49.
- [2] B.G. Yacobi, D.B. Holt, *Cathodoluminescence Microscopy of Inorganic Solids*, Plenum Press, New York, 1990, pp. 55–230.
- [3] V. Wittpahl, Y.Y. Liu, D.S.H. Chan, W.K. Chim, J.C.H. Phang, L.J. Balk, K.P. Yan, A degradation monitor for the light output of LEDs based on cathodoluminescence signals and junction ideality factor, 1996 IEEE International Reliability Physics Symposium, 29 April–2 May 1996, Dallas, TX, USA.
- [4] K.L. Pey, J.C.H. Phang, D.S.H. Chan, *Scanning Microscopy* 9 (2) (1995) 367–380.
- [5] D.B. Holt, D.C. Joy, *SEM Microcharacterization of Semiconductors*, Academic Press, London, pp. 241–338.
- [6] S.A.E. Johansson, J.L. Campbell, *PIXE: A Novel Technique for Elemental Analysis*, Wiley, Chichester, 1988.
- [7] W.-K. Chu, J.W. Mayer, M.A. Nicolet, *Backscattering Spectrometry*, Academic Press, New York, 1978.
- [8] M.B.H. Breese, P.J.C. King, G.W. Grime, F. Watt, *J. Appl. Phys.* 72 (6) (1992) 2097.
- [9] C. Yang, *Ionoluminescence techniques for geological applications*, Ph.D. Thesis, 1995.
- [10] C. Yang, K.G. Malmqvist, M. Elfman, P. Kristiansson, J. Pallon, K.A. Sjöland, R.J. Utui, *Nucl. Instr. and Meth. B* 130 (1997) 746.
- [11] J.F. Ziegler TRIM ver95, IBA-Research, Yorktown, NY 10598, 1995.